J. Fluid Mech. (1983), *vol.* 129, *pp.* 27–54
Printed in Great Britain

The characteristics of low-speed streaks in the near-wall region of a turbulent boundary layer

By C. R. SMITH AND S. P. METZLER
Department of Mechanical Engineering and Mechanics, Lehigh University, Bethlehem, PA 18015

(Received 2 September 1981 and in revised form 17 November 1982)

Employing a high-speed video system and hydrogen bubble-wire flow visualization, the characteristics of the low-speed streaks which occur in the near-wall region of turbulent boundary layers have been examined for a Reynolds-number range of $740 \leqslant Re_\theta < 5830$. The results indicate that the statistics of non-dimensional spanwise streak spacing are essentially invariant with Reynolds number, exhibiting consistent values of $\overline{\lambda^+} \approx 100$ and remarkably similar probability distributions conforming to lognormal behaviour. Further studies show that streak spacing increases with distance from the wall owing to a merging and intermittency process which occurs for $y^+ \gtrsim 5$. An additional observation is that, although low-speed streaks are not fixed in time and space, they demonstrate a tremendous persistence, often maintaining their integrity and reinforcing themselves for time periods up to an order of magnitude longer than the observed bursting times associated with wall region turbulence production. A mechanism for the formation of low-speed streaks is suggested which may explain both the observed merging behaviour and the streak persistence.

1. Introduction

One of the first clues to the existence of an ordered structure within a turbulent boundary layer was the discovery of an instantaneous spanwise velocity distribution consisting of alternating zones of high- and low-speed fluid which develop in the viscous sublayer and extend into the logarithmic region. Streamwise filaments of low-speed fluid (streaks) with a fairly uniform transverse spacing were observed in the near-wall region by Ferrell, Richardson & Beatty (1955). They flushed a turbulent pipe flow of coloured water with clear fluid and watched as the dye was swept from the outer portions of the boundary layer, leaving only streamwise traces of dyed fluid close to the wall. This phenomenon was discovered concurrently by Hama (see Corrsin 1956), who noted that, when dye was injected into the sublayer through a small slit in the wall, the marking agent became concentrated into narrow regions of low velocity. However, the first systematic investigation and quantification of the low-speed streak phenomena was done by Runstadler, Kline & Reynolds (1963), where it was first shown that the mean spacing between streaks could be quantified and correlated.

Since these initial studies, the streaky structure has been recognized and examined for a number of different experimental conditions. Kline *et al.* (1967) investigated boundary layers subject to different pressure gradients and noted the presence of the low-speed streak structure in all cases, even those in which relaminarization had begun to occur. A unique aspect of streaks is that they display a remarkable degree of persistence and regularity; even when disrupted, the streaky pattern quickly

re-establishes itself. The ubiquity of streaks has led Kline (1978) to propose that they constitute a universal feature of bounded shear flows and that the presence of streaks is a sufficient condition for establishing whether a given boundary-layer flow is turbulent.

The dominance of this type of spanwise phenomenon is also illustrated by the laminar boundary layer undergoing transition, where one of the first non-uniformities to be observed is a spanwise, sinusoidal variation in the mean velocity which has the appearance of what seems to be a precursor of the streaky structure (see Hama & Nutant 1963). This similarity between turbulent streaks and spanwise transition behaviour is particularly striking when one compares the hydrogen bubble-wire visualization pictures of Kline *et al.* (1967) in a fully turbulent boundary layer with those of Bippes (1972) obtained for a transitional boundary layer on a concave surface.

The importance and the significance of the low-speed streaks is that they act as apparent sites for the production of turbulent kinetic energy via a process identified by Kim, Kline & Reynolds (1971) as 'bursting'. During this process, individual low-speed streaks are described as lifting away from the wall, oscillating, and then breaking down (i.e. losing their coherence owing to an unstable interaction with surrounding higher-speed fluid) such that a substantial portion of the low-speed fluid is ejected into the outer flow. Kim has shown that this bursting of low-speed streaks contributes the majority of the turbulent kinetic energy produced in a turbulent boundary layer. Because of this apparently intimate relationship between low-speed streaks and turbulence production via the 'bursting' process, it seems clear that the physical characteristics of low-speed streaks should be a reflection of the physics giving rise to surface-transport processes such as surface drag and heat transfer (see e.g. Oldaker & Tiederman 1977) and thus merit close examination.

Various studies have examined the physical characteristics of the low-speed streaks, such as mean transverse spacing, and vertical and streamwise extent. For low-Reynolds-number flows ($Re_\theta < 1500$), the mean spanwise spacing between slow-speed streaks $\bar{\lambda}$ was initially established using primarily flow-visualization techniques (see Schraub & Kline 1965), and is generally accepted as $\overline{\lambda^+} = \bar{\lambda} u_\tau/\nu = 100 \pm 20$, where $\bar{\lambda}$ is the mean spanwise spacing between streaks, non-dimensionalized on the viscous length ν/u_τ. This value has been confirmed by several studies employing different visual and probe techniques to infer streak spacing (Oldaker & Tiederman 1977; Achia & Thompson 1976; Lee, Eckelmann & Hanratty 1974; Blackwelder & Eckelmann 1979; Kreplin & Eckelmann 1979; Nakagawa & Nezu 1981). However, for more developed flows, it has been speculated that a functional dependence upon Reynolds number may exist. Indeed, Gupta, Laufer & Kaplan (1971) and Haritonidis (1979), using a horizontal rake of hot-wire probes, have determined what seem to be larger $\overline{\lambda^+}$ values for higher Re_θ up to 10^4.

A limited examination of the variation of streak spacing with height was done by Schraub & Kline (1965), where it was shown, using both visual counting and correlation techniques, that streak spacing appears to increase for $y^+ \geqslant 7$; however, no explanation for this observed increase was offered. Nakagawa & Nezu (1981), in a series of low-Reynolds-number experiments using both visual techniques and hot-film probe-correlation techniques, showed an apparent increase in streak spacing for $y^+ > 10$, asymptoting to a value of $\overline{\lambda^+} \approx 2y^+$ for $y^+ > 100$.† They suggest that

† These higher y^+ values are based on results that exhibit a very weak spanwise scale. It is not clear that these values represent the spacing between well-defined low- (or high-) speed regions (i.e. streaks).

the increase in scale may be due to a pairing interaction of the low-speed streaks as they move outward from the wall, resulting in the increase in scale.

The length of the streak structures has been inferred from measurements performed by Blackwelder & Eckelmann (1979) in a low-Reynolds-number oil channel using a combination of hot-film probes and flush-mounted surface elements. They found apparently connected regions of low axial velocity in the region $5 \leqslant y^+ \leqslant 30$ that could be correlated for streamwise lengthscales extending beyond $\Delta x^+ > 1000$ in some cases. These findings were in essence confirmed in probe-correlation studies by Kreplin & Eckelmann (1979) using the same oil-channel facility. Dye studies by Oldaker & Tiederman (1977) also indicate that streaks may exceed $\Delta x^+ > 1000$; however, they could not visually follow a streak beyond the point where the streak was observed to 'burst' since this resulted in a dissipation of their visualization medium.

The present paper describes quantitative flow-visualization results obtained using a high-speed video flow-visualization system which allows the detailed visual examination of both the statistics and characteristics of low-speed streaks over a much wider range of Reynolds numbers than has been possible before. In addition, by use of a versatile hydrogen bubble-wire probe, a detailed examination of variations in streak-spacing statistics and characteristics with distance from a surface has been done for $y^+ < 30$.

2. Experimental apparatus

The facility used for the present study is a free-surface Plexiglas water-channel facility with a 5 m working section, 0·9 m wide by 0·3 m deep (shown in figure 1*a*). Utilizing a speed-control unit with a shaft speed feedback circuit, stable speeds from 0·01 m/s to 0·60 m/s may be attained. Using a combination of a 15 cm thick settling sponge (which covers the distribution manifold), flow-straightener–screen combination, and 5:1 inlet contraction, a turbulence intensity of 0·4 % at 0·3 m/s and a spanwise flow uniformity of $\pm 2\,\%$ are achieved. The boundary layers examined in this study were all tripped using a 2 mm diameter rod placed at the channel entrance to assure a consistent transition location. Using the boundary layer generated on the bottom surface of the channel, $Re_\theta \leqslant 4200$ can be achieved for 20 °C water. Using an auxiliary heating unit, water temperatures of 40 °C can be reached, which extends the Reynolds-number range to $Re_\theta \leqslant 6000$.

In order to determine the basic parameters of the turbulent boundary layers examined, a series of time-mean velocity and turbulence-intensity profiles were measured using a single-sensor hot-film anemometer system (DISA 55D01 with DISA 55M25 linearizer) for $770 < Re_\theta < 3100$. The velocity profiles obtained were then employed to determine δ, δ^*, θ, H and u_τ (by a Clauser cross-plot). The subsequent data were fitted to appropriate empirical correlations, and these correlations were used to establish the parameters for the visual studies. Although a range of Reynolds numbers was examined, typical results for an intermediate Reynolds number were $u_\infty = 0{\cdot}249$ m/s, $\nu = 0{\cdot}975 \times 10^{-6}$ m^2/s, $\delta \approx 10$ cm, $\delta^* = 1{\cdot}23$ cm, $\theta = 0{\cdot}89$ cm ($Re_\theta = 2270$), $u_\tau = 0{\cdot}0102$ m/s. Four of the mean-velocity profiles plotted in wall region form are shown in figure 2. Further details of both the flow system and anemometer measurements are given in Metzler (1980).

Visualization of the streak structure was done using a uniquely designed hydrogen-bubble-wire probe (described in Metzler 1980; Smith 1978) which allows a 25 μm diameter platinum wire, 20 cm in length, to be located parallel to the floor of the

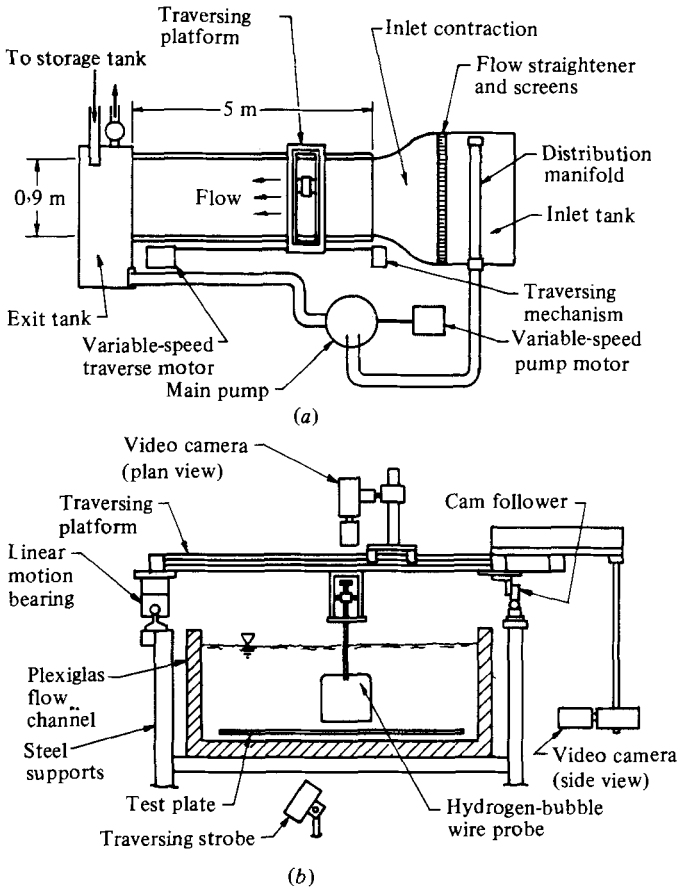

FIGURE 1. Free-surface water channel: (*a*) schematic of flow facility; (*b*) end-on view of channel (looking downstream) and traversing platform.

channel and transverse to the flow direction. The wire, used as the cathode in an electrolysis process, generates time lines of hydrogen bubbles through the use of a specially designed generator unit. Using this probe and a traversing unit, bubble lines can be introduced parallel to the floor of the channel at any desired height and at pulse rates from 0·2 to 340 Hz.

The video viewing and recording system is a two-camera high-speed closed-circuit system (manufactured by the Video Logic Corp.) which incorporates synchronized strobe lights to provide 120 frame/s with effective frame exposure time of 10 μs. This very short exposure time allows clear pictures to be obtained for highly magnified sequences with high relative motion. An exceptionally clear picture is obtained from the high-resolution screen using 250 horizontal direct-overlay rasters with a sweep frequency of 25·2 kHz. Using conventional lenses, fields of view as small as 6×6 mm can be obtained at distances of 0·5 m. A split-screen capability allows two different fields of view to be simultaneously displayed and recorded. All recorded data can be played in flicker-free slow motion (both forward and reverse), as well as single-framed for detailed data analysis. Figure 1 (*b*) is an end-view schematic of the flow-visualization system, configured for split-screen (plan-side) viewing of the streak structure. Note that the system mounts on a special traverse platform which allows the entire system to be positioned at any location along the channel length.

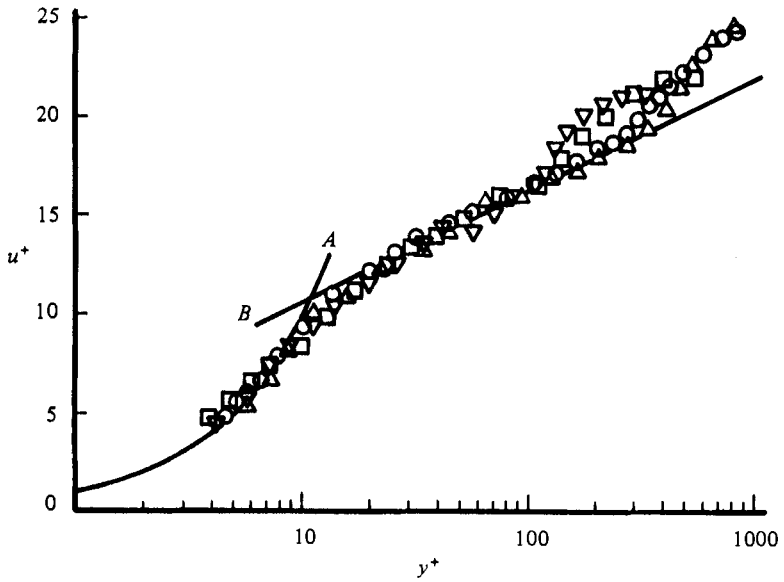

FIGURE 2. Mean-velocity distribution. Re_θ: ▽, 770; □, 1100; ○, 2270; △, 3100. *A*, $u^+ = y^+$; *B*, $u^+ = 2{\cdot}44 \ln y^+ + 5{\cdot}0$.

Once a video sequence is recorded, individual stop-action frames can be taken directly from the video screen using conventional photography or via a videographic copier which interfaces directly with the video recorder.

3. Experimental results

3.1. *Streak appearance*

Seven examples of stop-action frames of the streak structure obtained using the video flow-visualization system are shown in figure 3 for $740 \leqslant Re_\theta \leqslant 5830$. All pictures are plan views with the flow left to right and the hydrogen-bubble wire located normal to the flow at a non-dimensional distance of $y^+ = 5$ above the wall. Both the actual spanwise field of view and the spanwise distance equivalent to $\Delta z^+ = 100$ are indicated for each picture. In order to provide the best comparison of the near-wall behaviour, a conscious effort was made to select pictures for figure 3 that represented the streak behaviour during a predominantly quiescent period when the streaks are the most consistent in appearance. Each picture shown was printed directly using the videographic copier, which creates an exact linear image directly from the recorded analog signal.

Comparison of the pictures in figure 3 shows clearly that low-speed streaks do occur at higher Reynolds number and are essentially invariant in basic appearance with Reynolds number. The primary differences in appearance are a consequence of (i) variations in the hydrogen-bubble-line generation frequency and pulse width; (ii) lighting and light-level variations (with the degree of magnification); (iii) uncertainty in the vertical location of the bubble wire ($\delta y^+ = \pm 1$). Detailed observation of the video sequences from which the pictures in figure 3 were taken indicated that the dynamic behaviour of the streaks is also essentially invariant with Reynolds number (this will be discussed further in subsequent sections).

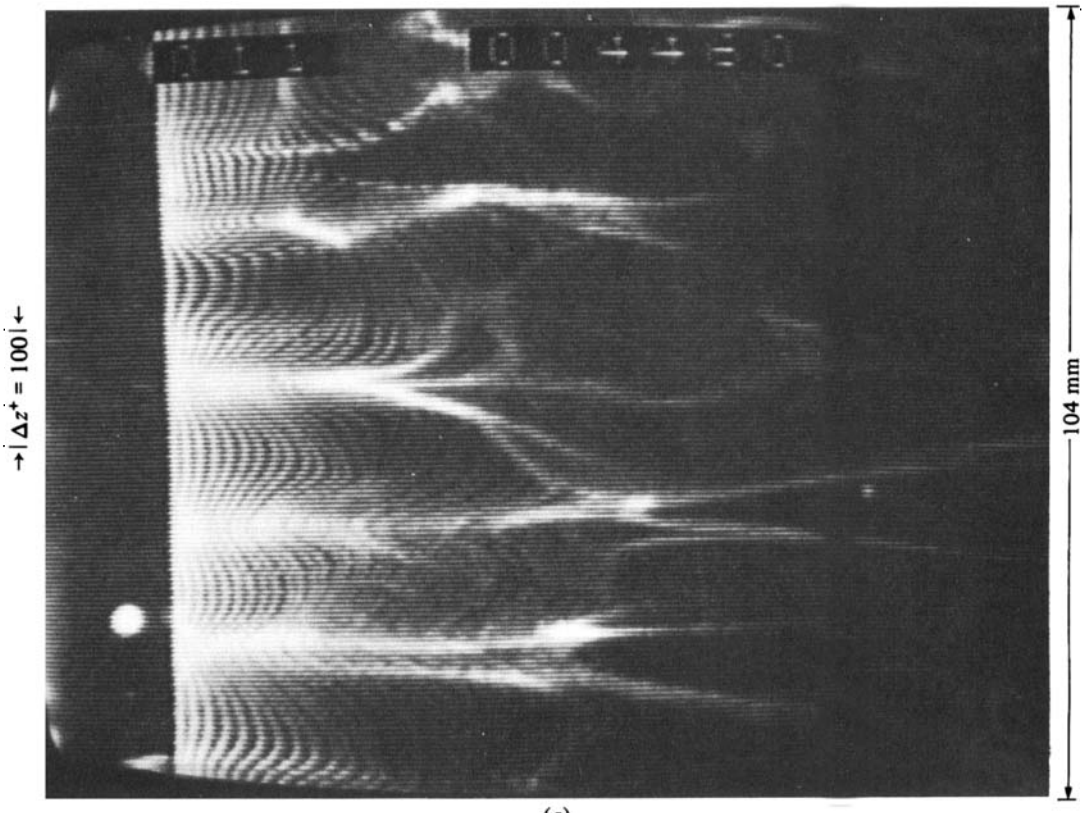

(*a*)

FIGURE 3(*a*). For caption see p. 35.

3.2. *Mean streak spacing*

The average spacing between low-speed streaks was determined for $740 \leqslant Re_\theta \leqslant 5830$. It is believed that this extends the upper range of Re_θ beyond that for which visually obtained values have been previously available. This also transcends a much broader range of Re_θ for which streak spacing has been visually documented on one experimental system. An additional facet of this study was the redundant measurement of the mean spacing for flows with essentially the same Re_θ, but differing free-stream velocity, viscosity, and location.

The streak-spacing values, presented in non-dimensional form $\lambda^+ = \lambda u_\tau/\nu$, were determined from visual identification using video sequences obtained with a horizontal hydrogen-bubble wire located at $y^+ \approx 5$. For each Reynolds-number setting, a video sequence of at least 7200 frames (1 min duration) was recorded. Lens magnification was set to give a quantifiable field of view of $\Delta x^+ \approx 900$ and $\Delta z^+ \approx 700$–800; the degree of magnification was determined by recording a short scene with a calibrated scale located adjacent to the bubble wire. Using the video recorder and videographic printer, a series of individual still pictures were obtained, with each picture spaced $\frac{5}{6}$ s (100 frames) apart. Typically 45–60 frames of data were evaluated for each video sequence. The span of time covered by each sequence of pictures represented a total sample duration (in terms of time T_B between turbulent bursts†) of approximately $20T_B$ for the lowest-velocity flow, and 100 T_B for the highest-velocity flow. At least 250 streaks were counted for each video sequence, yielding a worst-case relative uncertainty for $\overline{\lambda^+}$ of $\pm 8\%$ (95% confidence level).

† Where $T_B U_\infty/\delta = 5$ is used, as per suggestion of Kim *et al.* (1971).

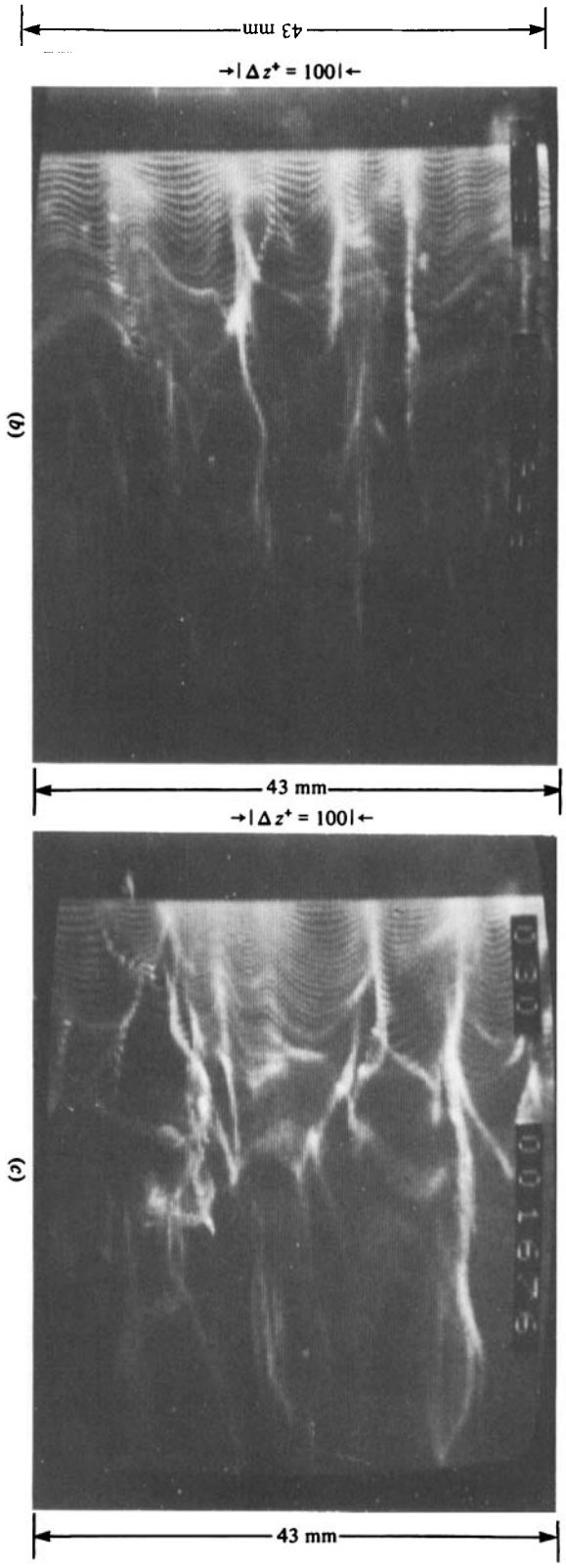

FIGURE 3 (*b*, *c*). For caption see p. 35.

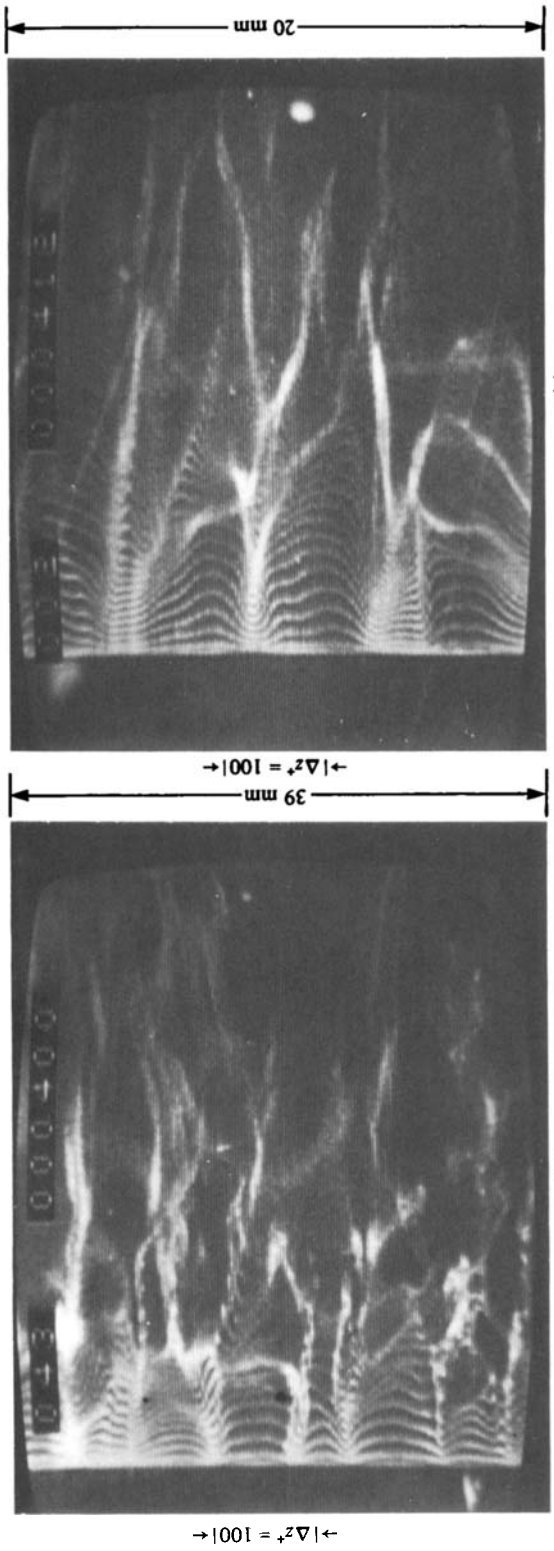

FIGURE 3 (*d*, *e*). For caption see facing page.

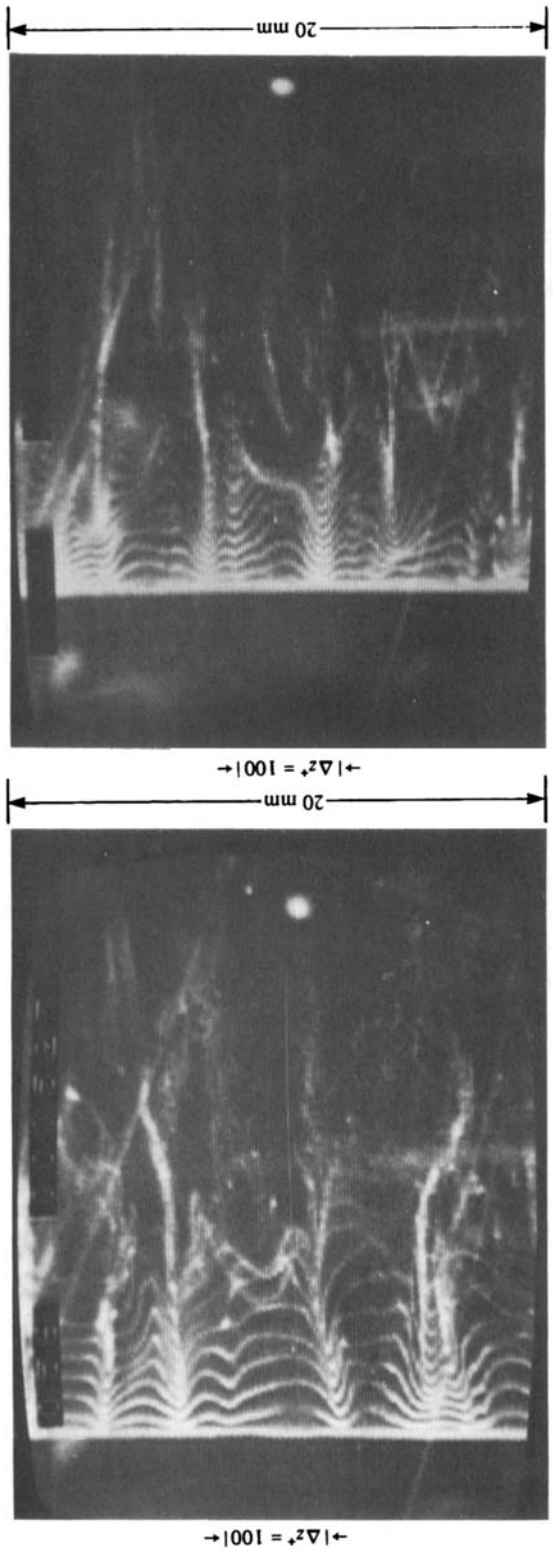

FIGURE 3. Plan views of low-speed streak patterns with spanwise hydrogen-bubble wire at $y^+ = 5$. (*a*) $Re_\theta = 740$, $f = 60$ Hz; (*b*) 1490, 120 Hz; (*c*) 2173, 120 Hz; (*d*) 3310, 120 Hz; (*e*) 4180, 240 Hz; (*f*) 4940, 240 Hz; (*g*) 5830, 340 Hz.

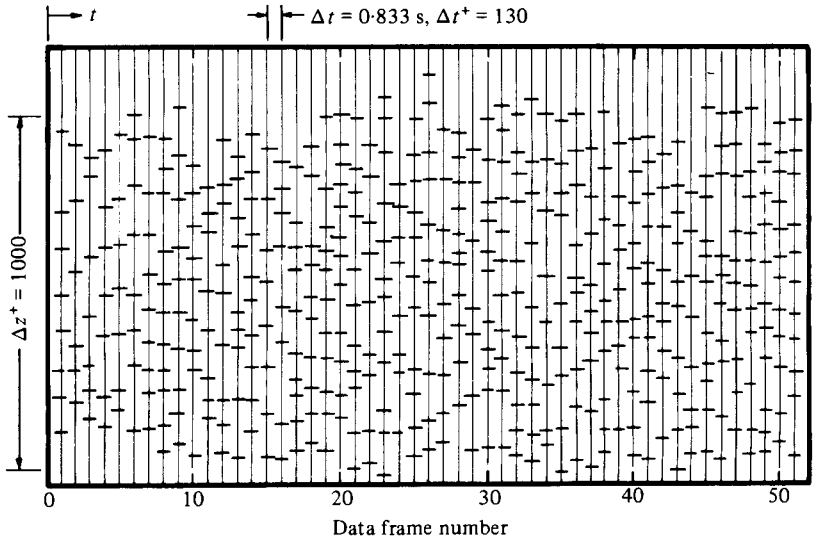

FIGURE 4. Streak-count transparency; $y^+ = 5$, $Re_\theta = 1490$.

The method for counting streaks required that three different individuals examine each series of videographic prints and perform independent streaks counts based upon a systematic set of counting rules. To allow a cross-comparison of the independent results, each counter marked each frame of data on a transparency printed with a series of spanwise axes offset in the time. When performing a streak count, the transparency was overlaid on each data frame and the location of each streak appearing in that frame was marked on the corresponding spanwise axis. After all data frames were marked by all counters, the transparencies were then compared and any noted discrepancies in identified streaks were discussed and resolved by reference to the actual video footage. The transparency data was then used to establish the mean streak spacing and (if desired) probability distributions. An example of a typical streak-count transparency is shown in figure 4. Note that each vertical line in the figure corresponds to one marked frame, and each small cross mark indicates the location of an identified streak.

The identification of a low-speed streak was done using the following method and criterion. A streamwise concentration of bubbles indicating an extended region of low streamwise velocity (closely spaced bubble lines) had to be present, well defined and with a streamwise extent of at least $\Delta x^+ = 100$. If a streak appeared to terminate, and its upstream end was more than $\Delta x^+ = 50$ downstream of the wire, it was not counted. There was no restriction on a minimum spanwise spacing; only if it appeared that the two streaks had completely merged (i.e. had no well-defined high-speed region between them, as described above) would they be counted as one. The location marked on the transparency was the transverse position of the streak $\Delta x^+ \approx 50$ downstream of the bubble wire.

Generally the identification of the low-speed regions was relatively straightforward since their length was well in excess of their spanwise spacing, and the differential in momentum flux between the adjacent high- and low-speed regions (determined by comparison of the local streamwise velocities) was quite dramatic, often in excess of 4 to 1. However, during the counting procedure, low-speed regions would be encountered which were weak or poorly developed. To establish whether these regions would be counted as a low-speed streak, it was required that the differential in

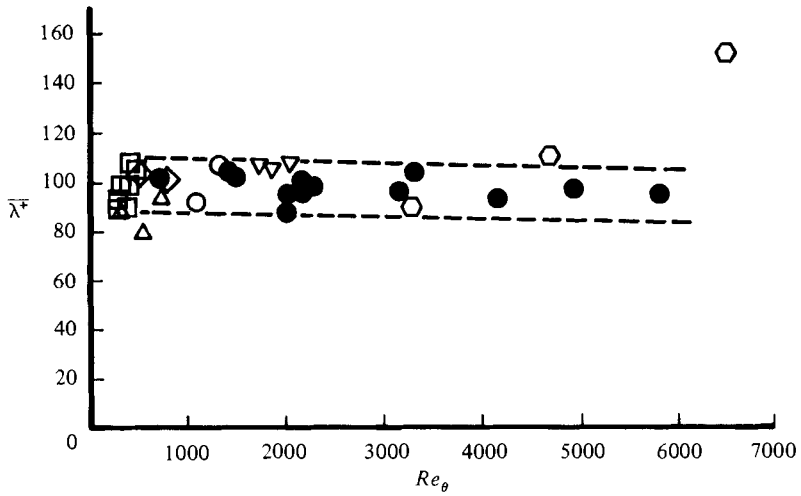

FIGURE 5. Mean non-dimensional streak spacing as a function of Reynolds number: ●, present study; ○, Schraub & Kline (1965); □, Oldaker & Tiederman (1977); ⬡, Gupta *et al.* (1971); △, Achia & Thompson (1976); ▽, Lee *et al.* (1974); ◇, Nakagawa & Nezu (1981); ---, $\pm 2\sigma$ interval about linear-regression fit to data of present study.

momentum flux between the adjacent high and low-speed regions be at least 2 to 1, or approximately one-half the ratio exhibited by a well-developed low-speed streak. Since the local momentum flux is roughly proportional to the square of the streamwise velocity, a 2 to 1 momentum flux differential required that $u_{\text{low}}/u_{\text{high}} < 0{\cdot}70$, as determined from the bubble-line pictures. To examine how this criterion might bias the streak-counting procedure, the acceptance criterion for $u_{\text{low}}/u_{\text{high}}$ was set respectively at 0·58, 0·70 and 0·82 (momentum-flux differentials of 3, 2 and 1·5) and separate streak counts were made for both the lowest and highest Reynolds-number data sequences. The results showed that $\overline{\lambda^+}$ increased approximately 4% for $u_{\text{low}}/u_{\text{high}} = 0{\cdot}58$ and decreased approximately 3% for $u_{\text{low}}/u_{\text{high}} = 0{\cdot}82$ relative to the $u_{\text{low}}/u_{\text{high}} = 0{\cdot}70$ values. It was thus judged that the acceptance criterion has only a weak effect on the overall streak-counting process, and at worst introduces a one-sided bias which is much smaller than the general uncertainty of the streak-counting procedure.

Figure 5 presents the mean streak spacing obtained in this investigation versus Re_θ; values obtained in previous studies are also shown for comparison. In table 1 the type of system and the parameters of the flows for which the data of figure 5 were obtained are also listed, when available. As shown in figure 5, the present results show no marked change in non-dimensionalized mean spacing $\overline{\lambda^+}$ for the Reynolds-number range examined. The results indicate that within the uncertainty of the data $\overline{\lambda^+}$ appears essentially independent of Reynolds number. This would appear consistent with previous visual studies, and indicates that the generally accepted mean value of $\overline{\lambda^+} \approx 100$ may be a universal number.

Two points of inconsistency with the above results are the higher-Reynolds-number data of Gupta *et al.* (1971) and some preliminary results by Haritonidis (1979), where hot-wire anemometry measurements at high Re_θ have indicated values larger than $\overline{\lambda^+} \approx 100$ for mean streak spacing. The experimental technique used in both these studies employs a transverse array of closely spaced hot-wire probe elements and ensemble averages of either correlation or spectral-type analyses to yield information regarding the scale associated with spanwise variations in the streamwise velocity.

Investigators	Re_θ	u_∞ (m/s)	u_τ (m/s)	x (m)†	ν (m²/s) $\times 10^6$	$\overline{\lambda^+}$
Present Study	740	0·121	0·0057	2·51	1·020	101
(flat plate, water)	1450	0·166	0·0071	4·27	1·050	104
hydrogen bubbles, $y^+ = 5$	1490	0·282	0·0122	2·51	1·025	102
	2020	0·221	0·0094	4·24	0·942	87
	2030	0·256	0·0107	3·87	0·989	95
	2170	0·189	0·0078	4·27	0·744	100
	2190	0·274	0·0113	4·27	1·067	96
	2260	0·314	0·0130	2·51	0·693	98
	3160	0·390	0·0155	4·50	1·032	96
	3310	0·305	0·0121	4·27	0·724	104
	4180	0·387	0·0150	4·27	0·695	93
	4940	0·475	0·0181	4·27	0·698	97
	5830	0·582	0·0220	4·27	0·702	95
Oldaker & Tiederman (1977)	298	0·169	0·0118	—	1·08	93
(channel flow, water)	312	0·180	0·0106	—	0·92	89
dye slot	312	0·174	0·0102	—	0·82	99
	373	0·335	0·0186	—	1·33	105
	404	0·287	0·0156	—	1·32	108
	402	0·174	0·0102	—	0·82	88
	480	0·174	0·1020	—	0·82	99
Gupta *et al.* (1971)	2200	—	0·1402	—	14·7	97·5
(flat plate, air)	3300	—	0·2256	—	14·8	89
probe rake,	4700	—	0·3277	—	14·8	110
$y^+ = 2$–7	6500	—	0·4511	—	14·8	151
Schraub & Kline (1965)	1080	0·152	0·0070	3·14	0·94	91
(flat plate, water)	1325	0·152	0·0069	4·11	0·89	106
hydrogen bubbles, $y^+ = 4$						
Achia & Thompson (1976)	327‡	0·249	0·0152	—	1·0	88
(pipe flow, water)	545‡	0·415	0·0245	—	1·0	79
hologram interferometry	725‡	0·553	0·0325	—	1·0	93
Lee *et al.* (1974)	1735‡	—	—	—	—	106
(pipe flow, chemical	1860‡	—	—	—	—	105
solution)	2045‡	—	—	—	—	107
electrochemical correlations						
Nakagawa & Nezu (1981)	750‡	0·100	0·0050	—	1·044	100
(fully developed,	500‡	0·066	0·0033	—	1·044	103
open-channel flow) hydrogen bubbles, $y^+ = 4$						

† Location from inlet. ‡ Estimated values.

TABLE 1. Mean streak spacing and flow parameters

A possible difficulty in interpreting these results as reflective of the true mean streak spacing is that the high-velocity air flows necessary to attain high Re_θ also possess small lengthscales (and thus streak spacing), some of which may not have been resolvable with the probe spacing used. This difficulty was recognized and commented on by Gupta *et al.* (1971), who determined a value of $\overline{\lambda^+} = 151$ for $Re_\theta = 6500$. It has also been pointed out by Schraub & Kline (1965) that, if they evaluated the same data set (quantified hydrogen-bubble time-streak markers) using both visual counting

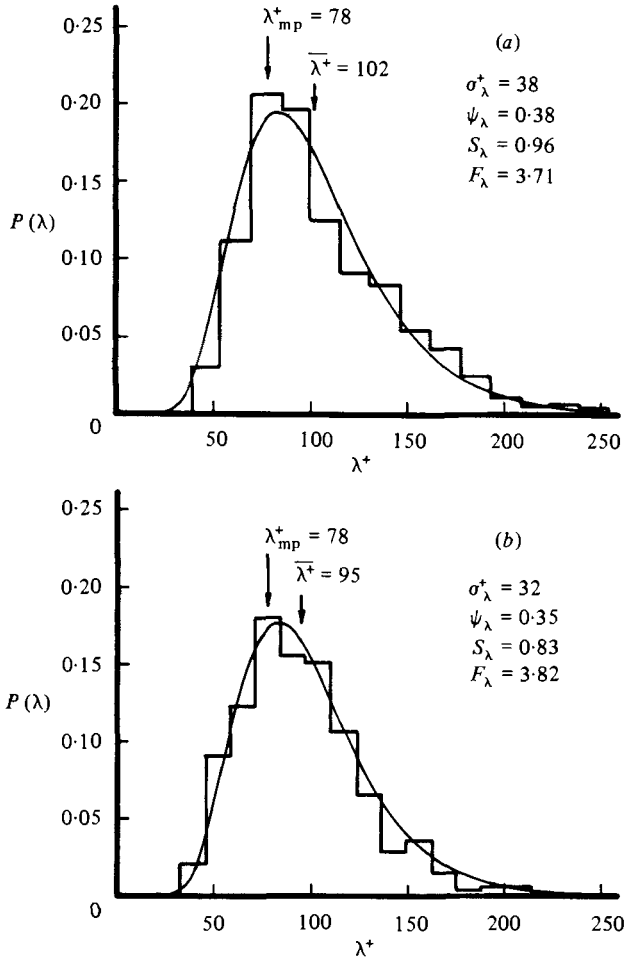

FIGURE 6. Probability-density histograms of spanwise streak spacing at $y^+ = 5$: (*a*) $Re_\theta = 1490$, $n = 437$; (*b*) $Re_\theta = 5830, n = 411$; ——, lognormal probability density distribution for corresponding λ^+ and ψ_λ.

and correlation techniques, the mean streak spacing obtained using the correlation techniques was generally 30 % larger than that obtained using visual techniques. This result was felt to be a consequence of the narrowness of the data window, and the inclusion of all spanwise scale effects, not just the sharp regions of velocity defect characteristic of the low-speed streaks.

3.3. *Spanwise distribution of streaks*

In order to examine the spanwise distribution of low-speed streaks, the marked streak count transparencies were used to establish distribution histograms as shown in figure 6. The two distributions shown in this figure were both established at $y^+ = 5$, but for Reynolds numbers differing by a factor of 4. As can be observed, the distributions appear to be very similar, skewed toward values lower than the mean. The distributions are similar to λ^+ distributions determined by Oldaker & Tiederman (1977) using dye-visualization techniques and by Lee *et al.* (1974) using electrochemical sensors. Note that in figure 6 the most-probable values of λ^+ are about 20 % less than the mean value, which agrees with the findings of Kline *et al.* (1967) for Reynolds numbers consistent with figure 6(*a*).

In order to characterize the streak spacing distributions statistically, the standard deviation, the coefficient of variation, the skewness and the flatness were determined using

$$\sigma_\lambda = \left[\frac{1}{n-1}\sum_{i=1}^{n}(\lambda_i-\bar{\lambda})^2\right]^{\frac{1}{2}} \quad \text{(standard deviation)}, \tag{1}$$

$$\psi_\lambda = \frac{\sigma_\lambda}{\bar{\lambda}} \quad \text{(coefficient of variation)}, \tag{2}$$

$$S_\lambda = \frac{\frac{1}{n-1}\sum_{i=1}^{n}(\lambda_i-\bar{\lambda})^3}{\sigma_\lambda^3} \quad \text{(skewness)}, \tag{3}$$

$$F_\lambda = \frac{\frac{1}{n-1}\sum_{i=1}^{n}(\lambda_i-\bar{\lambda})^4}{\sigma_\lambda^4} \quad \text{(flatness)}, \tag{4}$$

with respective values indicated for each distribution in figure 6. Comparison of the statistical properties indicates the two distributions to be essentially identical with moderate positive skewness and slightly more peaked than a Gaussian distribution ($F_\lambda = 3{\cdot}0$). λ^+ distributions determined at $y^+ = 5$ for 6 other Reynolds numbers gave results essentially identical with those shown in figure 6, demonstrating skewness and flatness values in the ranges $0{\cdot}75 < S_\lambda < 1{\cdot}0$ and $3{\cdot}5 < F_\lambda < 4{\cdot}0$. The range of ψ_λ for all 8 streak distributions examined was $0{\cdot}34 < \psi < 0{\cdot}40$, which is consistent with a value of 0·36 determined by Oldaker & Tiederman (1977). Estimates for ψ_λ of 0·30–0·40 by Schraub & Kline (1965) and 0·40 by Gupta *et al.* (1977) are also similar to the values of the present study.

On the basis of low-Reynolds-number ($Re_\theta < 750$) channel-flow studies, Nakagawa & Nezu (1981) have suggested that the spanwise spacing of low-speed streaks may be represented by a lognormal distribution (i.e. where the *logarithm* of the streak spacing is normally distributed). For the present study this form of probability density function is given by

$$P(\lambda) = \frac{\exp\left\{-\frac{1}{2}\left(\frac{1}{\psi_0}\ln\frac{\lambda}{\lambda_0}\right)^2\right\}}{\lambda\psi_0(2\pi)^{\frac{1}{2}}} \tag{5}$$

where

$$\lambda_0 = \bar{\lambda}(1+\psi_\lambda^2)^{-\frac{1}{2}}, \tag{6}$$

$$\psi_0 = [\ln(1+\psi_\lambda^2)]^{\frac{1}{2}}. \tag{7}$$

Here λ_0 represents the median value of λ, and ψ_0 is the coefficient of variation of $\ln\lambda$ (see Hastings & Peacock 1975). Employing (5), lognormal probability density distributions were determined for the appropriate $\bar{\lambda}$ and ψ_λ values and superposed over the corresponding histograms in figure 6. The comparison for both distributions appears quite good considering the finite sample size for the histograms ($n \approx 400$).

To verify further the lognormal behaviour of streak spacing, the data of figure 6 were replotted in figure 7 on a lognormal probability graph of $\alpha(\lambda)$ versus $\log(\lambda/\bar{\lambda})$, where

$$\alpha(\lambda) = \frac{\int_0^\lambda P(\lambda)\,d\lambda}{\int_0^\infty P(\lambda)\,d\lambda}. \tag{8}$$

Figure 7 shows the streak spacing distributions to be essentially lognormal (indicated by a straight-line probability graph); the corresponding probability graph for a true

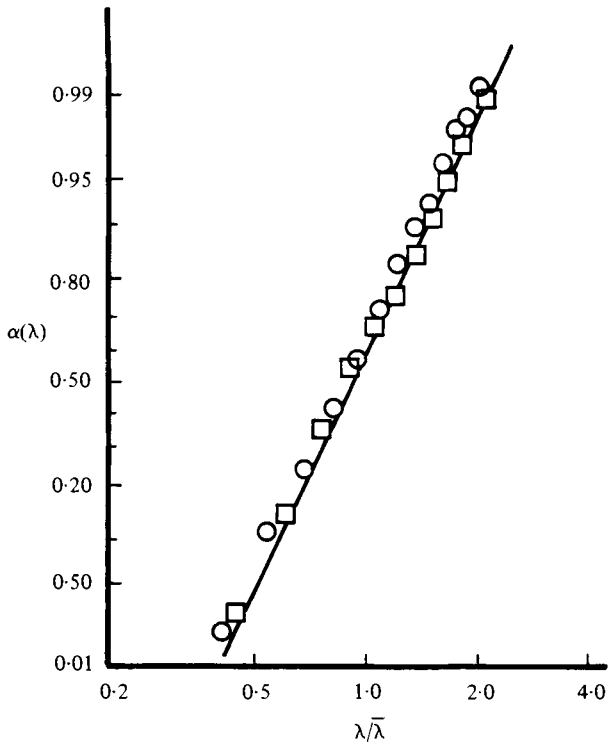

FIGURE 7. Lognormal probability graph of spanwise streak spacing at $y^+ = 5$: □, $Re_\theta = 1490$; ○, $Re_\theta = 5830$; ——, lognormal probability distribution for $\psi_\lambda = 0{\cdot}38$.

lognormal distribution with $\psi_\lambda = 0{\cdot}38$ is shown for comparison, indicating very good agreement with the $Re_\theta = 1490$ data. The λ^+ distributions obtained for six other Reynolds numbers were also shown to demonstrate the same lognormal behaviour.

For a true lognormal distribution, the ratio of the most-probable value to the mean value can be shown to be (see Hastings & Peacock 1975),

$$\frac{\lambda_{\mathrm{mp}}}{\bar{\lambda}} = (1+\psi_\lambda^2)^{-\frac{3}{2}}. \tag{9}$$

For the range $0{\cdot}34 \leqslant \psi_\lambda \leqslant 0{\cdot}40$ determined in the present study, (9) yields $0{\cdot}85 < \lambda_{\mathrm{amp}}/\bar{\lambda} < 0{\cdot}80$, which is (as pointed out previously) almost identical with the ratio demonstrated by the present distributions and that quoted by Kline *et al.* (1967).

Thus, in the very-near-wall region ($y^+ = 5$) it appears that (i) spanwise streak spacings conform closely to a lognormal distribution, as suggested by Nakagawa & Nezu (1981), and (ii) the distribution is essentially invariant with Reynolds number up to at least $Re_\theta = 6000$, and most probably in general.

The apparent adherence of the streak spacings to a lognormal distribution can be tentatively explained as follows (see Aitchison & Brown 1957). First, the impossibility of negative values of λ requires that all values be positive, but with a potentially unconstrained upper limit. Secondly, one must recognize that the distribution of a random variable (in this case λ) about its mean value is the result of a large number of independent influences, each of which produces a small effect on the value of that variable. In the case of a normally distributed variable, each influence will be

independent of the magnitude of the variable itself. However, a random variable will develop a lognormal distribution when the independent influences cause variations which are *proportional* to the variable. As a comparative example, personal incomes are distributed lognormally owing to such income-proportional influences as interest rates, taxes, etc. Thus the lognormal distribution of spanwise streak spacing would seem to indicate that the independent physical influences which affect the variations in streak spacing are in some manner dependent upon the relative values of the streak spacing itself.

3.4. *Streak persistence*

During the performance of streak counts using the overlay transparencies, it was noted that streaks would often tend to persist for periods of time much longer than accepted bursting times. Referring back to figure 4, the evidence of this persistence can be observed as a pattern of sinuous 'lines' into which the marks locating the streaks in time t^+ and space z^+ appear to arrange themselves. Upon close scrutiny of figure 4 one can see that the 'lines' are neither regular nor of consistent length (in time), but it is clear that a persistence of location exists such that the streaks do not rearrange themselves in a totally random fashion between subsequent time intervals. Review of all the other streak-counting transparencies showed this same pattern of persistence to be present regardless of Reynolds number.

In order to verify further this pattern of persistence, the videotape from which figure 4 was obtained was reviewed frame-by-frame to determine whether the apparent persistence is a true continuation or reinforcement of an existing streak, or simply a chance occurrence. At each streak-counting interval, the videotape was used to determine if each marked streak location could be related to a previously marked streak location. Generally, the frame-by-frame tracking of each streak was a straightforward process since streaks do not move rapidly in a lateral direction. A continuation of a streak was judged to occur if a low-speed region satisfying the criteria for streak identification at the beginning of a streak-counting interval either (i) maintained that criteria over the entire streak-counting interval or (ii) ceased to satisfy the identification criteria, but an identifiable velocity-defect region remained which could be tracked frame-by-frame and observed to evolve into a region which again satisfied the streak-identification criterion before the end of the streak-counting interval. If a streak continuation occurred, the counting marks were connected by a line, thus indicating the persistence of the low-speed streak.† This process was then repeated for each marked streak location on the streak-counting transpareney. The end result of this examination is figure 8, which is a series of lines in time and space indicating streak persistence, i.e. the tendency of individual streaks, as identified visually in a fixed reference frame, to either (i) maintain their integrity through repeated reinforcement or (ii) contribute to the initiation of a new streak. As can be observed from figure 8, many of the streaks appear to have a substantial persistence; the average streak persistence for the data shown is $\Delta t_p^+ = \Delta t_p u_\tau^2/\nu \approx 480$, with several streaks persisting for times as long as $\Delta t_p^+ = 2500$. Note that a pattern of streak persistence very similar to that of figure 8 was obtained by Utami & Ueno (1979) for turbulent flow in a shallow channel. Unfortunately they did not document their conditions sufficiently for comparison with the present results.

Several points should be clarified regarding the nature of the streak persistence. First, all the streaks observed in this study were subject to the classical 'bursting' behaviour which results in the quasi-periodic ejection of fluid from the streak into

† Note that, if a streak appeared to split or merge, this was indicated by a 'branching'.

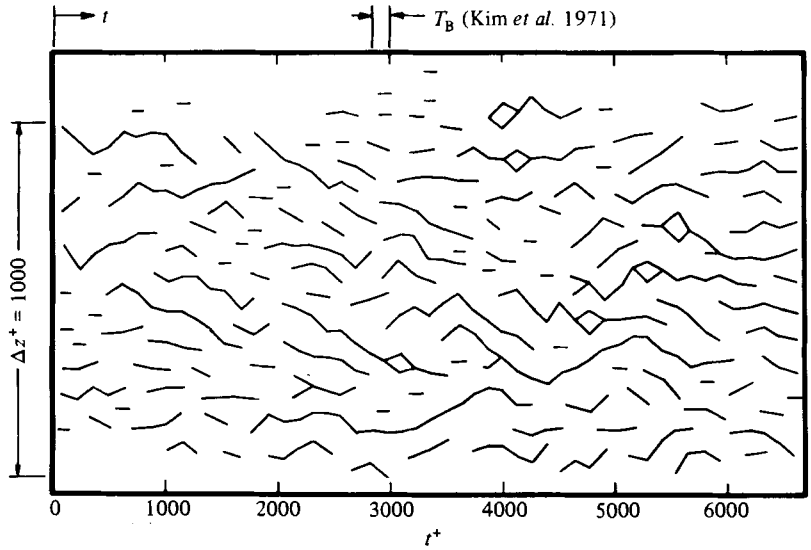

FIGURE 8. Streak-persistence graph as determined from figure 4 and review of original video sequence; $y^+ = 5$, $Re_\theta = 1490$.

the outer region of the boundary layer. It was observed, however, that, when a streak 'bursts', a certain residual amount of low-speed fluid will generally remain on the wall, which can be observed to result in the reformation and reinforcement of the old streak or initiation of a new streak. This continual reformation of an existing streak or initiation of a new low-speed streak in proximity to a previous streak is the process of persistence. In fact (as can be observed in figure 8), it was less common for a streak to appear spontaneously than it was for it to have a traceable genealogy.

Secondly, it is important to note that what persists is the *region* of low-speed fluid, not a specific mass of fluid. It is the continual accretion of low-momentum fluid into the streak which maintains its presence, not a specific mass of fluid convecting with the flow. This can be thought of as similar to the dynamics of a separated flow where the separated region occupies a reasonably definable region in space, but the fluid within the region is continually exchanged with the mainstream fluid by a complex shedding–accretion process. In fact Offen & Kline (1975) have suggested that streaks may be conceptualized as local separations when viewed from a moving reference frame; the moving-reference studies of Smith (1978) support this concept.

A third point to be made is that, although streaks are persistent, they are not spacially fixed. As shown by figure 8, the location of persistent streaks can vary strongly in the spanwise direction, indicating that the persistence is not tied to any irregularity of the test system. To examine whether the persistence of streaks affects their random distribution in time and space, spanwise distribution histograms of streak location were established using several of the marked transparencies. Figure 9 is an example of a histogram of the spatial distribution of low-speed streaks over time as determined from the data of figure 4. The results indicate that, despite their persistence, streaks do become randomly distributed over a sufficient time period. However, the times required to achieve this spanwise randomness are quite long. For example, the coefficient of variation of the spanwise distribution of the data shown in figure 9 is still $\pm 4{\cdot}2\,\%$ for a sample time of 42 s ($\Delta t^+ = 6500$). This is consistent with similar results of Shraub & Kline (1965) (see also Kline 1967), who suggest that the lengthy time interval over which randomness is achieved is the reason that long

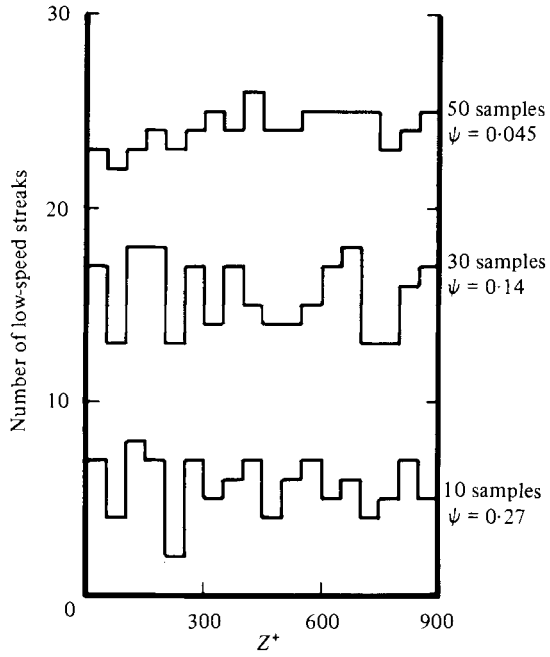

FIGURE 9. Spatial distribution of low-speed streaks showing effect of sample size; $y^+ = 5$, $Re_\theta = 1490$.

integration times are required to achieve stable mean values of flow properties in the near-wall region. Note that this problem is not nearly as noticeable in air flows, where, for a similar Reynolds number at $U_\infty = 10$ m/s, $\Delta t^+ = 6500$ would represent only 0·50 s.

3.5. *Variations in streak spacing with distance from surface*

To examine variations in λ^+ with distance from a surface, distribution histograms of non-dimensional streak spacing were determined for $Re_\theta = 2030$ at six different distances from the surface out to $y^+ = 30$. The six histograms shown in figure 10 were compiled following the same streak-identification constraints as outlined previously, and represent sequences of approximately 400 streak samples per histogram. To ensure absolute consistency of conditions, all six sequences were taken within a 20 min time period, varying only the vertical position of the bubble wire while holding all other conditions (including lighting) constant.

The two most apparent characteristics illustrated by figure 10 are (i) increased mean streak spacing for $y^+ \gtrsim 5$, and (ii) a broadening of the streak distribution with increased distance from the wall. Figure 11 clearly shows an increase in $\overline{\lambda^+}$ and σ_λ^+ (indicative of a broadening of the distribution) with increasing y^+. Data points for $\overline{\lambda^+}$ determined by Schraub & Kline (1965) and Nakagawa & Nezu (1981) at lower Reynolds numbers are also shown for comparison, and appear to be in essential agreement with the present results. Figure 11 indicates that $\overline{\lambda^+}$ is approximately constant in the very-near-wall region ($y^+ \lesssim 5$), consistent with observations by Oldaker & Tiederman (1977). For $y^+ > 10$, $\overline{\lambda^+}$ appears to scale monotonically as the edge of the logarithmic zone (law of the wall) is approached. This behaviour appears to be consistent with the requirement that the lengthscales of the shear stress producing motions be proportional to y^+ in the wall region. Beyond $y^+ = 30$ the streaks were not sufficiently well defined to warrant making streak counts; however, qualitative observation of the data indicated that the dominant spanwise scale

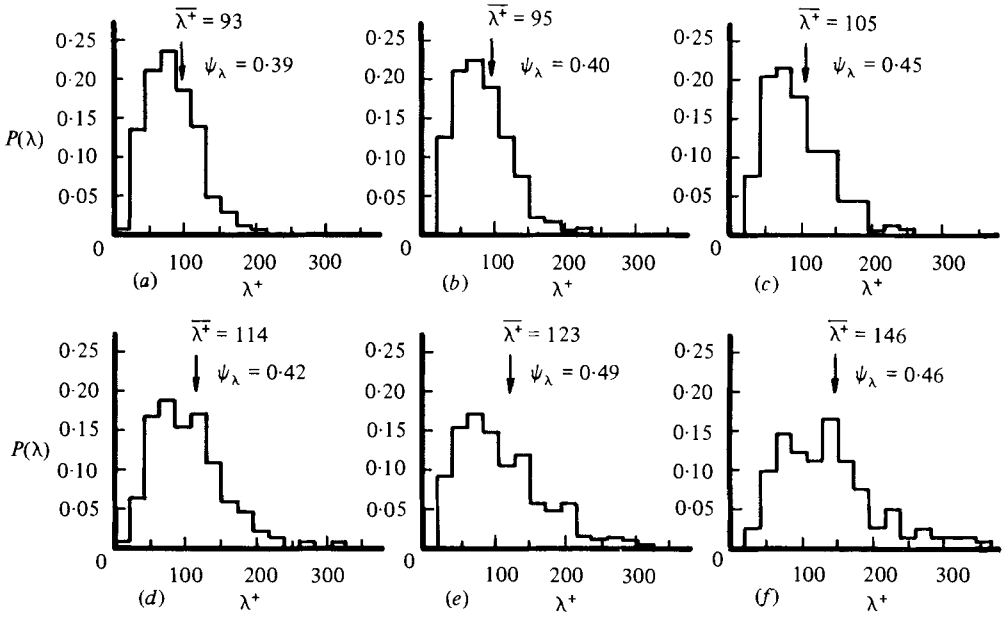

FIGURE 10. Probability-density histograms of spanwise streak spacing for $Re_\theta = 2030$: (*a*) $y^+ = 1$; (*b*) 5; (*c*) 10; (*d*) 15; (*e*) 20; (*f*) 30.

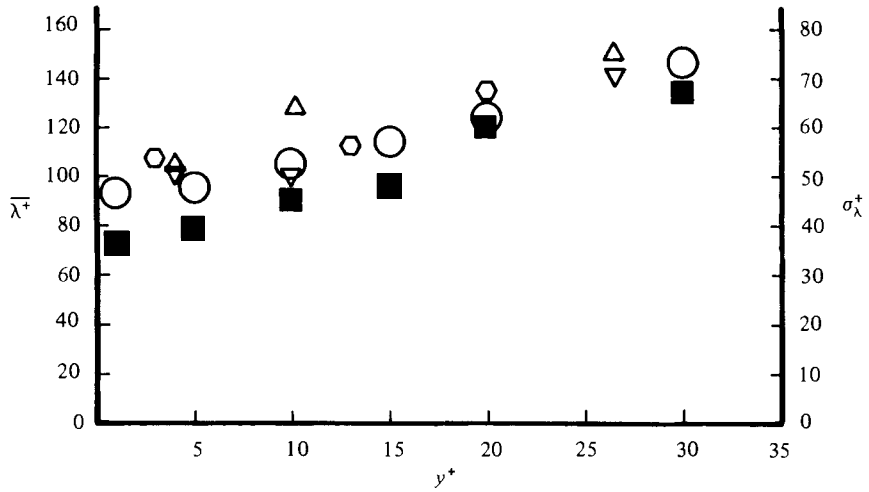

FIGURE 11. Variation of mean spanwise streak spacing and standard deviation with distance from wall. Present study: ○, $\overline{\lambda^+}$, $Re_\theta = 2030$; ■, σ_λ^+, $Re_\theta = 2030$. Schraub & Kline (1965): ○, $\overline{\lambda^+}$, $Re_\theta = 1325$. Nakagawa & Nezu (1981): △, $\overline{\lambda^+}$, $Re_\theta = 830$; ▽, $\overline{\lambda^+}$, $Re_\theta = 500$.

appears to increase with increased distance from the wall. This is consistent with probe-correlation studies of Nakagawa & Nezu (1981), who indicate that the dominant spanwise scale of the bursting behaviour appears to be proportional to y^+ (for $y^+ > 50$). However, there is some question as to whether the spanwise scale they determined corresponds to the well-defined streaks of the present study or some other more-mature coherent structure to which the low-speed regions near the wall (and the mechanism for their generation) are contributory.

The relative change in the streak-spacing distributions of figure 10 is illustrated by figure 12, which shows the respective coefficient of variation, skewness, and

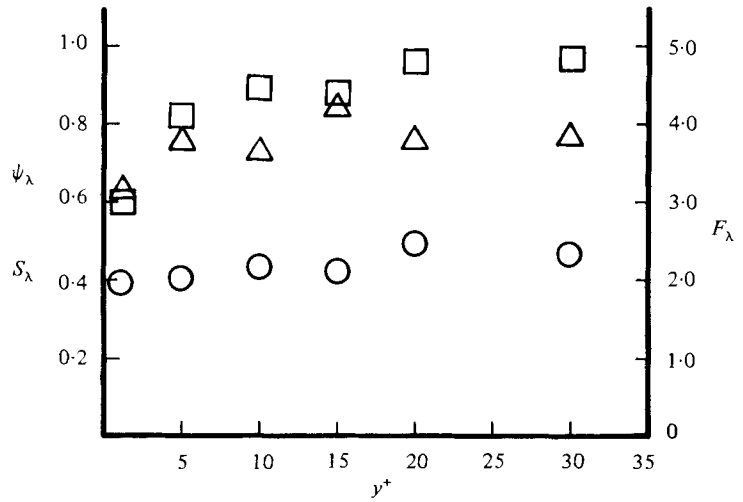

FIGURE 12. Coefficient of variation, skewness and flatness for streak spacing histograms of figure 10: ○, ψ_λ; □, S_λ; △, F_λ.

flatness for each distribution. These results indicate that, despite a substantial broadening of the streak spacing with increasing y^+, the distributions undergo very little change in character. They remain positively skewed and only slightly peaked, with the largest changes in S_λ and F_λ occurring between $y^+ = 1$ and $y^+ = 5$. The modest increase in ψ_λ with y^+ is indicative of a small relative growth of the number of values at the extremes of the distribution (essentially at the larger spacings for the present distributions). This increase in larger spanwise scales is a result of a process of streak merging and intermittency, which will be discussed subsequently.

The applicability of the lognormal distribution for spanwise streak spacing away from the wall was examined by replotting the histogram data of figure 10 on a lognormal probability graph as shown in figure 13. To facilitate comparison, a true lognormal distribution for $\psi_\lambda = 0{\cdot}42$ is also shown. Although the streak-spacing histograms appear to vary from true lognormal behaviour at the extremes of the graph, they appear consistent with lognormal behaviour over most of the central range, $0{\cdot}15 < \alpha(\lambda) < 0{\cdot}95$. This is most reflective of (i) the actual histograms being a bit broader about the median values than the lognormal distribution, and (ii) a possible bias toward lower streak spacings due to the finite observation window ($\Delta z^+ \approx 800$). Comparison of the skewness and flatness of the histograms with those obtained for a true lognormal distribution yielding the same ψ_λ appears to bear out these points. For example, at $y^+ = 30$ the streak-spacing histogram yields $\psi_\lambda = 0{\cdot}46$, $S_\lambda = 0{\cdot}96$ and $F_\lambda = 3{\cdot}80$. By comparison, a true lognormal distribution with $\psi_\lambda = 0{\cdot}46$ yields $S_\lambda = 1{\cdot}48$ and $F_\lambda = 7{\cdot}10$. Thus the true lognormal distribution is more positively skewed (owing to a longer high-end tail) and more peaked. Despite these discrepancies, the lognormal distribution does appear to sufficiently represent the shape and characteristics of the streak-spacing histograms such that it may be considered at least an approximate model of the low-speed streak spacing in the region $1 < y^+ < 30$.

3.6. *Streak merging and intermittency*

In order to understand the process or processes that result in the observed increase of $\overline{\lambda^+}$ with distance from the surface, a detailed slow-motion study was done of all original video sequences plus additional sequences employing fields of view as small

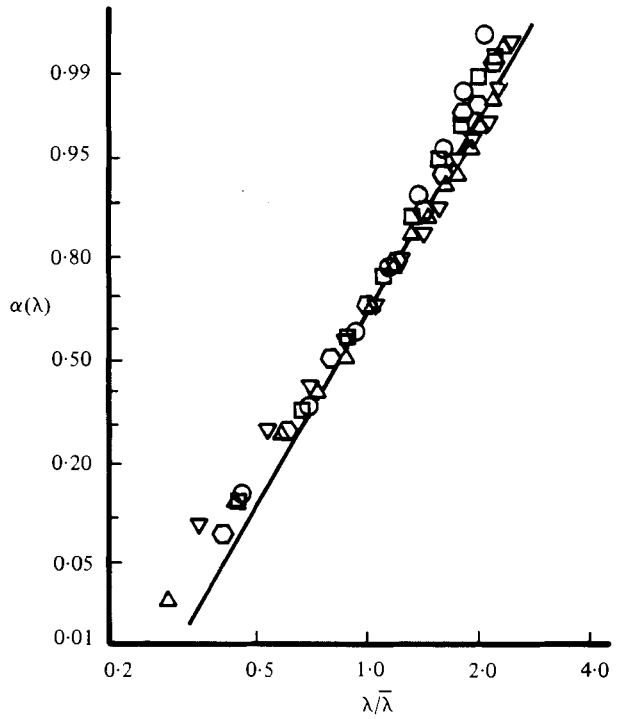

FIGURE 13. Lognormal probability graph of spanwise streak spacing for $Re_\theta = 2030$; ○, $y^+ = 1$; □, 5; ○, 10; ▽, 20; △, 30; ——, lognormal probability distribution for $\psi_\lambda = 0{\cdot}42$.

as $\Delta z^+ \approx 300$. From this examination it was determined that with the bubble wire located at $y^+ < 5$ the low-speed streaks appear as low-speed regions of typical streamwise extent of $\Delta x^+ > 1000$ which seldom merge or interact strongly. As the bubble wire is moved farther from the surface ($y^+ \geqslant 5$), two phenomena are observed which give rise to a larger perceived streak spacing. The first of these is streak merging or coalescence, which begins to occur for $y^+ \geqslant 5$ and is most pronounced for $10 \leqslant y^+ \leqslant 30$. The effect of this merging process is to consolidate and reduce the number of independent low-speed regions in the flow.

Figure 14 is a series of 4 plan-view pictures, obtained with a bubble wire at $y^+ = 30$, which illustrate the appearance of the merging behaviour. This sequence of pictures, which spans a time of $\Delta t^+ = 24$, shows four low-speed streaklike regions with an initial spanwise spacing between streaks of $\lambda^+ \approx 100$ merging into the low-speed regions with $\lambda^+ \approx 200$. Note the expanded low-speed regions downstream of the merged streaks (figure 14*d*), and what appears to be the presence of streamwise vortices (labelled V1, V2, V3 in figure 14*c*) as evidenced by the 'kinking' in the time lines. After repeated observation of many such merging events exhibiting the same essential characteristics, it is suggested that this behaviour is the result of small stretched and lifted vortex loops generated in the very-near-wall region and interacting strongly as they move away from the wall. The streamwise vortices are construed as the stretched legs of these vortex loops which are moving together and away from the wall due to mutual-induction effects. The potential presence of vortex loops in the near-wall region will be addressed further in §4.

In addition to merging, a process of streak division could also be observed, particularly for $y^+ \leqslant 15$. As viewed in a fixed reference frame, several streaks would often be observed to merge temporarily, and then subsequently separate again into

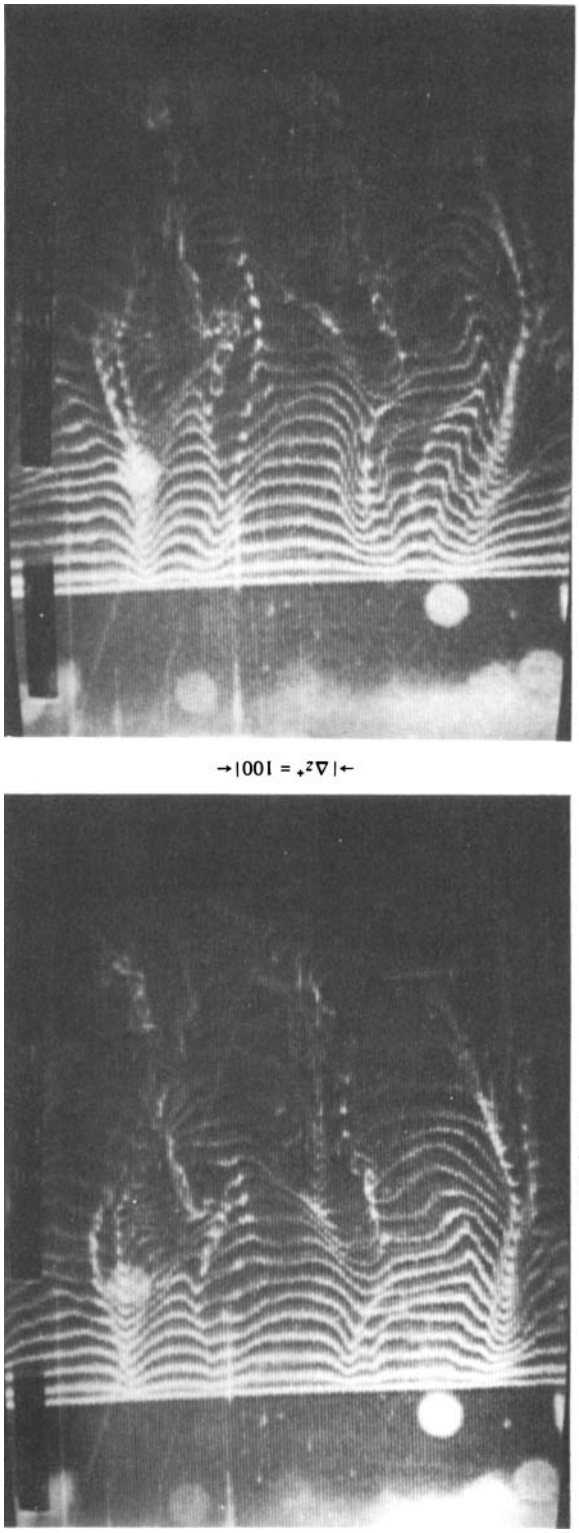

FIGURE 14 (*a*, *b*). For caption see facing page.

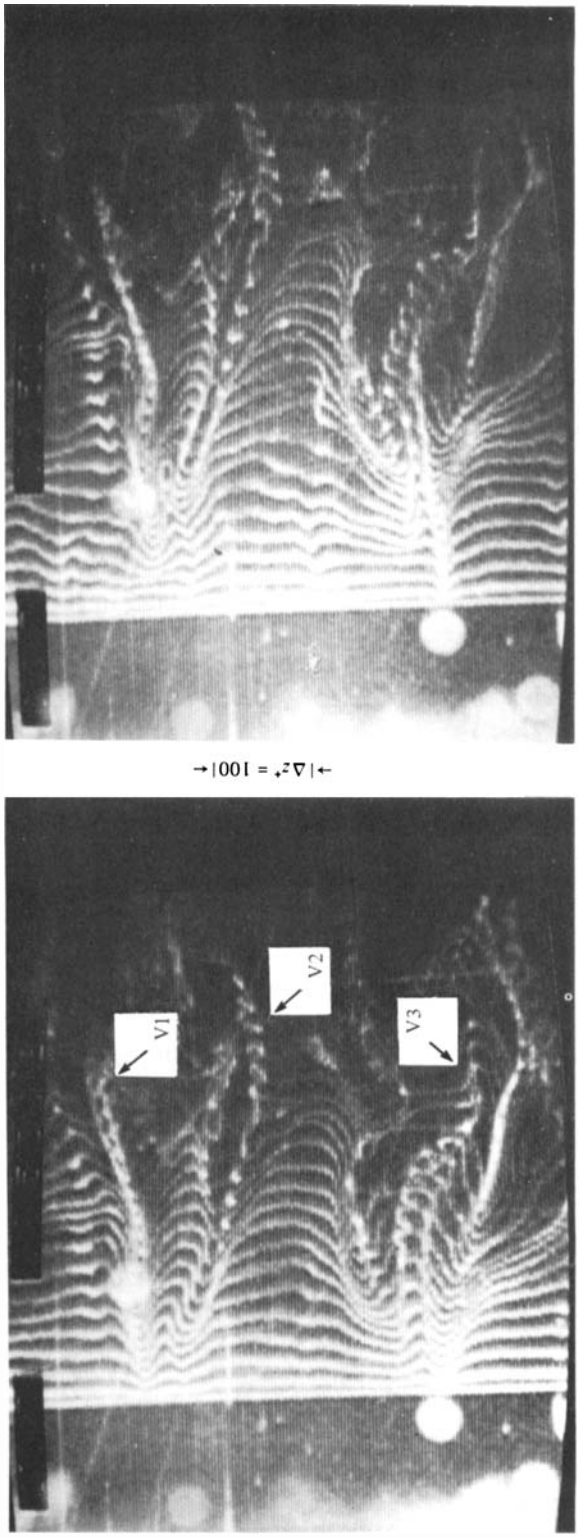

FIGURE 14. Plan view of low-speed streak pattern illustrating merging behaviour; $Re_\theta = 2190$, $y^+ = 30$, $f = 120$ Hz.

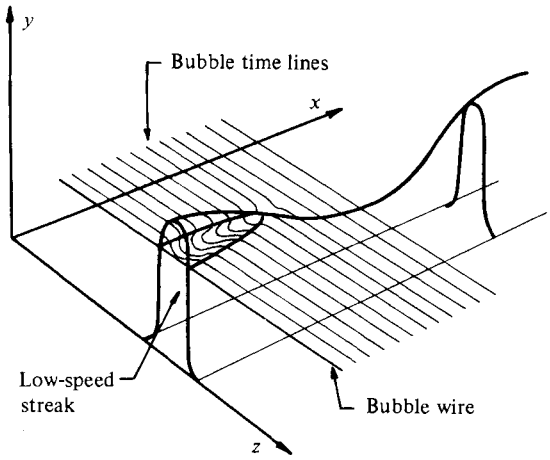

FIGURE 15. An illustration of how 'undulations' of a low-speed streak give rise to an apparent intermittency of the streak when visualized with a spanwise hydrogen-bubble wire.

(apparently) the original constituent streaks. In those cases, only part of the streamwise length of a given streak appeared to be involved in the merging process.

This process of streak merging and division has been observed and commented on previously by Nakagawa & Nezu (1981). They suggest that very near the wall ($y^+ \leqslant 5$) streaks continually combine and divide in essential equilibrium, which keeps $\overline{\lambda^+}$ constant. They speculate that the inrush of fluid occurring during a sweep motion is responsible for the division of the streaks, and, since the strength of the inrush weakens away from the wall, fewer streak divisions would occur. This decrease in streak division with distance from the wall was speculated to allow the coalescence process to dominate, which would result in an increased $\overline{\lambda^+}$. The present higher-Reynolds-number studies indicate that it is an increase in streak coalescence, not a decrease in streak division, which results in increased $\overline{\lambda^+}$; and, in contrast with the results of Nakagawa & Nezu, the division of a streak, when it occurred, could not be correlated with an inrush behaviour, nor could it necessarily be related to the bursting behaviour of the streak.

Another phenomenon resulting in a lower streak count, and thus larger $\overline{\lambda^+}$, was the apparent disappearance and reappearance of single streaks. This intermittency process was generally observed for $y^+ \geqslant 20$, and appeared to result from 'humps', or undulations, in the upper edge of the region of low-speed fluid defining a streak. Figure 15 illustrates how this undulation in the low-speed region manifests itself as a 'disappearing' streak when viewed using a horizontal bubble wire.

The overall effects of both the streak merging and intermittency phenomena are (i) to create an increasingly disrupted and intermittent streak pattern, (ii) to decrease the number of defineable streaks per unit width (and thus increase $\overline{\lambda^+}$), and (iii) to decrease the overall length of low-speed streaks (as visualized using a bubble wire) to $\Delta x^+ \approx 100$ for $y^+ > 30$.

The histograms presented in figure 10 can be used to illustrate the effect of streak merging and intermittency on observed streak spacing with distance from the surface. For $y^+ = 1$ and $y^+ = 5$ (figures 10*a*, *b*) the distributions both peak about $\lambda^+_{\mathrm{mp}} \approx 75$. As y^+ is increased ($y^+ = 10$, figure 10*c*), λ^+_{mp} remains essentially the same, but decreases in probability. This decrease in probability is hypothesized to be the result of merging of these most-probable streaks to yield larger streaks of approximately twice the spacing ($\lambda^+ \approx 150$) and thus a broader distribution. For y^+ farther from the

wall ($y^+ = 15$ and 20, figures 10*d*, *e*), streak merging becomes very pronounced, further spreading the distribution toward $\lambda^+ \approx 150$ and reducing the percentage of $\lambda^+_{mp} \approx 75$ streaks even further. In addition, intermittent streak behaviour leaves 'gaps', which result in a significant increase in the upper extreme of the distribution. Finally, as y^+ is increased to 30 (figure 10*f*), λ^+_{mp} jumps to approximately 145, as streak merging below this y^+ level produces a much wider streak spacing, which combined with increased intermittency drives the upper extreme of the distribution even higher. Note that the distribution in figure 10(*f*) appears to be somewhat double-peaked, appearing to reflect both the initial streak spacing in the sublayer region and the merged or coalesced spacing predominating farther from the wall.

As pointed out previously, increases in spanwise spacing are to be expected since both dimensional analysis and the universality of the logarithmic shape of the mean-velocity profiles indicate that the lengthscale of the turbulent structure in the wall region ($y^+ \gtrsim 30$) should scale with y^+. The present data indicated that beyond the viscous sublayer ($y^+ \approx 5$) the streak spacing does appear to asymptote toward a linear scaling with distance from the wall. It is also worth noting that the region $10 < y^+ < 20$, which appears to demonstrate the most-active merging behaviour, is also the region of maximum production of turbulent energy. The implication of this observation is that the observed merging process may be either a result of or possibly contributory to the turbulence-production process.

4. Summary and discussion

The results of the visualization study presented here indicate that the statistical characteristics of the spanwise spacing of low-speed streaks are essentially invariant with Reynolds number, exhibiting consistent values of $\overline{\lambda^+} \approx 100$ and remarkably similar probability distributions over an eightfold range in Re_θ. In addition, the basic appearance of low-speed streaks is observed to be essentially identical for all Reynolds numbers examined (see figure 3). An increase in $\overline{\lambda^+}$ and a broadening of the probability distributions for $y^+ \geqslant 5$ appear to be the results of both a merging or coalescence of the very-near wall streaks ($y^+ \leqslant 5$) and an intermittency effect due to undulations in the upper extent of the low-speed regions constituting the streak.

It has been shown that near the wall ($y^+ \leqslant 5$) spanwise streak distributions are peaked with $\lambda^+_{mp} \approx 75$–80. Since streak spacing is low-end limited, the process of merging appears to result in a reduction of the number of these most-probable streaks and a subsequent increase in streaks with spacing of the order of $2\lambda^+_{mp}$ and higher (see figure 14). The effect of this process was clearly demonstrated in the sequence of distributions shown in figure 10. This increase in identifiable spanwise scale can also be observed in the previous pictures of Schraub & Kline (1965) and Runstadler *et al.* (1963) (see also Kline *et al.* 1967). Taken to its natural conclusion, one would expect the process of merging to continue into regions farther from the wall than examined here, yielding even larger spanwise scales; indeed the low-Reynolds-number studies of Nakagawa & Nezu (1981) indicate that the spanwise scales associated with the bursting phenomena appear to increase with y^+ well into the outer wall region, as the scaling of the logarithmic region dictates they should. However, for $y^+ \geqslant 30$ streak identification becomes very uncertain, such that a process of systematic visual streak counting becomes too subjective. The difficulty appears to be that the streak-merging and coalescence process becomes very three-dimensional away from the surface. Thus, at some distance from the wall, extended coherent regions of low-speed fluid cease to exist, as the low-speed streaks pass through a metamorphosis

yielding a more complex flow pattern. Kline (1978) suggests $y^+ \approx 40$ as the upper limit for which well-defined streaks can be identified; the present study would concur with this value. Thus a structure that is coherent and clearly identifiable very near the wall will become much less coherent and describable as the structure moves away from the wall and interacts in a very complex process with other low-speed regions. A comparison of figures 3 and 14 illustrates this change in complexity quite well.

The persistence of streaks observed in the present study is not a new observation, having been qualitatively observed and commented on before (Runstadler *et al.* 1963; Schraub & Kline 1965; Smith 1978; Utami & Ueno 1979). A unique observation of the present study is that the streak persistence appears to far exceed the conventional burst times, thus indicating that streaks must undergo a strong process of perpetuation. An explanation for streak persistence can be found in a study by Smith & Metzler (1982) using simultaneous plan-side views of a horizontal hydrogen-bubble wire of narrow spanwise extent. They observed that the breakdown of a streak during the bursting process appears to be associated with the formation of a series of stretched loop or hairpin-type vortices in the near-wall region (the initial stages of this loop-formation process appear to have been characterized by Kim *et al.* (1971) as the oscillation of a streak prior to bursting). As these loops (formed such that each leg of the loop straddles the streak) are convected away from the surface, a strong vortex-stretching process occurs in the streamwise direction which causes the legs of the vortices to appear as counter-rotating vortex pairs which act to reinforce the streak, and thus create the appearance of streak persistence. Repeated loop formation during streak bursting would create a situation of continued reinforcement of the streak, which could explain the extreme persistence of some streaks. In addition, since the stretching of the streamwise vortices near the wall should have a stabilizing effect (Saffman & Baker 1979) the resultant streak should maintain its integrity far downstream, as has been determined in previous studies.

The formation of stretched vortex loops in the near-wall region is not a unique concept, having been suggested before by Kline *et al.* (1967), Willmarth & Tu (1967), Offen & Kline (1975), Hinze (1975), Head & Bandyopadhyay (1978), Smith (1978), Utami & Ueno (1979) and Wallace (1982). In fact Hinze provides a mechanistic picture similar to that proposed above in regard to the loop-formation–streak-reinforcement process. Further, in a study showing great insight, Head & Bandyopadhay (1981) provide convincing evidence for not only the existence but also the dominance of stretched loop vortices (or hairpin vortices as they term them) in turbulent boundary layers. Their model details the characteristics of the more mature, developed vortex loops and essentially complements the study by Smith & Metzler, which examines the origin and development of the vortex loops. Finally, a recent visual study by Perry, Lim & Teh (1981) using a smoke sheet in a wind tunnel has produced pictures which seem to show clearly that a turbulent spot is formed by the organized development and evolution of an agglomeration of loop vortices.

Evidence supporting the presence of streamwise counter-rotating vortex pairs in the near-wall region has been presented by Schraub & Kline (1965), Bakewell & Lumley (1967), Kastrinakis *et al.* (1978), Smith (1978), Blackwelder & Eckelmann (1979), Kreplin & Eckelmann (1979), Utami *et al.* (1982) and Head & Bandyopadhay (1981). And, in a recent visual study, Schwartz (1981) (see also Smith *et al.* 1982) used simultaneous plan-end view studies of a hydrogen-bubble wire to show both the presence of counter-rotating structures in the near-wall of turbulent boundary layers and their apparent relationship to the streak-formation process.

As mentioned previously, the presence of stretched loop vortices near the surface

could also explain the observed streak-merging behaviour that occurs for $y^+ > 5$. Since the streak-breakdown process must be influenced by interaction with the multiscale outer-region flow, it is speculated that this could result in a distribution of loop vortices in the near-wall region which vary in location, scale, strength and degree of development. The resultant interaction of such a distribution of loop vortices would be a complex process dominated by vortex stretching and viscous interaction near the wall where mean velocity gradients are large, changing to inviscid-type vortex coalescence and mutual-induction effects farther from the wall where mean velocity gradients diminish. Thus, for $y^+ \gtrsim 10$, where the mean-velocity gradient is less than 25 % of the wall value, one would anticipate that inviscid-type vortex interactions would begin to predominate, becoming more and more dominant, complicated and three-dimensional the farther from the wall and the weaker the mean-velocity gradient (which is responsible for intensifying the streamwise vorticity by stretching). Specific evidence from the present study which appears to support such an interacting vortex-loop scenario are (i) the apparent merging of the low-speed streaks, (ii) the increase in effective spanwise scale and decrease in longitudinal scale of the low-speed regions, and (iii) the increasing complexity of the flow appearance, all of which occur as distance from the wall is increased.

The authors wish to thank J. B. Johansen and S. P. Schwartz for their assistance in the data-acquisition and reduction process. Funding of this work by the Air Force Office of Scientific Research, Washington, D.C., is gratefully acknowledged.

REFERENCES

ACHIA, B. U. & THOMPSON, D. W. 1976 *J. Fluid Mech.* **81**, 439.

AITCHISON, J. & BROWN, J. A. C. 1957 *The Lognormal Distribution*. Cambridge University Press.

BAKEWELL, H. P. & LUMLEY, J. L. 1967 *Phys. Fluids* **10**, 9.

BIPPES, H. 1972 Experimentelle Untersuchung des laminar-turbulenten Umschlags an einer parallel angeströmten konkaven Wand. *Sitz. Heidelberger Akad. Wiss. Math.-naturwiss. Klasse* **3**, 103.

BLACKWELDER, R. F. & ECKELMANN, H. 1979 *J. Fluid Mech.* **94**, 577.

CORRSIN, S. In *Proc. 1st Symp. on Naval Hydrodyn. N.A.S.–N.R.C. Publ.* 515, p. 373.

FERRELL, J. K., RICHARDSON, F. M. & BEATTY, K. O. 1955 *Ind. Engng Chem.* **47**, 29.

GUPTA, A. K., LAUFER, J. & KAPLAN, R. E. 1971 *J. Fluid Mech.* **50**, 493.

HAMA, F. R. & NUTANT, J. 1963 In *Proc. 1963 Heat Transfer and Fluid Mech. Inst.*, vol. 77. Stanford University Press.

HARITONIDAS, J. H. 1979 *Bull. Am. Phys. Soc.* **24**, 1142.

HASTINGS, N. I. J. & PEACOCK, J. B. 1975 *Statistical Distributions*, p. 84. Butterworth.

HEAD, M. R. & BANDYOPADHYAY, P. 1978 In *Coherent Structure of Turbulent Boundary Layers* (ed. C. R. Smith & D. E. Abbott), p. 98. AFOSR/Lehigh University Workshop, Dept Mech. Engng & Mech., Bethlehem, PA.

HEAD, M. R. & BANDYOPADHAY, P. 1981 *J. Fluid Mech.* **107**, 297.

HINZE, J. O. 1975 *Turbulence*, p. 683. McGraw-Hill.

KASTRINAKIS, E. G., WALLACE, J. M., WILLMARTH, W. W., GHORASHI, B. & BRODKEY, R. S. 1978 In *Structure and Mechanisms of Turbulence I* (ed. H. Fiedler). Lecture Notes in Physics, vol. 75, p. 175.

KIM, H. T., KLINE, S. J. & REYNOLDS, W. C. 1971 *J. Fluid Mech.* **50**, 133.

KLINE, S. J. 1967 In *Fluid Mechanics of Internal Flow* (ed. F. Sovran), p. 27. Elsevier.

KLINE, S. J. 1978 In *Coherent Structure of Turbulent Boundary Layers* (ed. C. R. Smith & D. E. Abbott), p. 1. AFOSR/Lehigh University Workshop, Dept Mech. Engng & Mech., Bethlehem, PA.

KLINE, S. J., REYNOLDS, W. C., SCHRAUB, F. A. & RUNSTADLER, P. W. 1967 *J. Fluid Mech.* **30**, 741.

KREPLIN, H. P. & ECKELMANN, H. 1979 *J. Fluid Mech.* **95**, 305.

LEE, M. K., ECKELMAN, L. D. & HANRATTY, T. J. 1974 *J. Fluid Mech.* **66**, 17.

METZLER, S. P. 1980 Processes in the wall region of a turbulent boundary layer. M.S. thesis, Dept of Mech. Engng & Mech., Lehigh University.

NAKAGAWA, H. & NEZU, I. 1981 *J. Fluid Mech.* **104**, 1.

OFFEN, G. R. & KLINE, S. J. 1975 *J. Fluid Mech.* **70**, 209.

OLDAKER, D. K. & TIEDERMAN, W. G. 1977 *Phys. Fluids Suppl. II* **20**, S133.

PERRY, A. E., LIM, T. T. & TEH, E. W. 1981 *J. Fluid Mech.* **104**, 387.

RUNSTADLER, P. W., KLINE, S. J. & REYNOLDS, W. C. 1963 *Dept Mech. Engng, Stanford University, Rep.* MD-8.

SAFFMAN, P. C. & BAKER, G. R. 1979 *Ann. Rev. Fluid Mech.* **11**, 95.

SCHRAUB, F. A. & KLINE, S. J. 1965 *Dept Mech. Engng, Stanford University, Rep.* MD-12.

SCHWARTZ, S. P. 1981 Investigation of vortical motions in the inner region of a turbulent boundary layer. M.S. thesis, Dept Mech. Engng & Mech., Lehigh University.

SMITH, C. R. 1978 In *Coherent Structure of Turbulent Boundary Layers* (ed. C. R. Smith & D. E. Abbott), p. 50. AFOSR/Lehigh University Workshop, Dept Mech. Engng & Mech., Bethlehem, PA.

SMITH, C. R. & METZLER, S. P. 1982 In *Developments in Theoretical and Applied Mechanics*, vol. XI (ed. T. J. Chung & G. R. Karr), p. 533. Dept Mech. Engng, University of Alabama in Huntsville.

SMITH, C. R., SCHWARTZ, S. P., METZLER, S. P. & CERRA, A. W. 1981 In *Flow Visualization II* (ed. W. Merzkirch), p. 605. Hemisphere.

UTAMI, T. & UENO, T. 1979 In *Flow Visualization* (ed. T. Asanunra), p. 221. Hemisphere.

UTAMI, T., UENO, T., IMAMOTO, H. & OHTOSHI, K. 1982 In *Flow Visualization II* (ed. W. Merzkirch), p. 476. Hemisphere.

WALLACE, J. M. 1982 In *Developments in Theoretical and Applied Mechanics*, vol. XI (ed. T. J. Chung & G. R. Karr), p. 509. Dept Mech. Engng, University of Alabama in Huntsville.

WILLMARTH, W. W. & TU, B. J. 1967 *Phys. Fluids Suppl.* **10**, S134.